NeuroImage 55 (2011) 1566–1576

Contents lists available at ScienceDirect

NeuroImage

journal homepage: www.elsevier.com/locate/ynimg

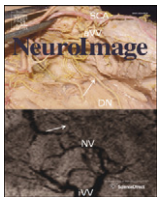

Partial volume effect as a hidden covariate in DTI analyses

Sjoerd B. Vos [a,*], Derek K. Jones [b], Max A. Viergever [a], Alexander Leemans [a]

[a] Image Sciences Institute, Department of Radiology, University Medical Center Utrecht, Utrecht, The Netherlands
[b] CUBRIC, Cardiff University Brain Research Imaging Centre, School of Psychology, Cardiff University, Cardiff, UK

ARTICLE INFO

Article history:
Received 9 September 2010
Revised 30 November 2010
Accepted 14 January 2011
Available online 22 January 2011

Keywords:
Diffusion tensor imaging
Fiber tractography
Partial volume effect
Hidden covariate
Aging

ABSTRACT

During the last decade, diffusion tensor imaging (DTI) has been used extensively to investigate microstructural properties of white matter fiber pathways. In many of these DTI-based studies, fiber tractography has been used to infer relationships between bundle-specific mean DTI metrics and measures-of-interest (e.g., when studying diffusion changes related to age, cognitive performance, etc.) or to assess potential differences between populations (e.g., comparing males *vs.* females, healthy *vs.* diseased subjects, etc.). As partial volume effects (PVEs) are known to affect tractography and, subsequently, the estimated DTI measures sampled along these reconstructed tracts in an adverse way, it is important to gain insight into potential confounding factors that may modulate this PVE. For instance, for thicker fiber bundles, the contribution of PVE-contaminated voxels to the mean metric for the entire fiber bundle will be smaller, and vice-versa — which means that the extent of PVE-contamination will vary from bundle to bundle. With the growing popularity of tractography-based methods in both fundamental research and clinical applications, it is of paramount importance to examine the presence of PVE-related covariates, such as thickness, orientation, curvature, and shape of a fiber bundle, and to investigate the extent to which these hidden confounds affect diffusion measures. To test the hypothesis that these PVE-related covariates modulate DTI metrics depending on the shape of a bundle, we performed simulations with synthetic diffusion phantoms and analyzed bundle-specific DTI measures of the cingulum and the corpus callosum in 55 healthy subjects. Our results indicate that the estimated bundle-specific mean values of diffusion metrics, including the frequently used fractional anisotropy and mean diffusivity, were indeed modulated by fiber bundle thickness, orientation, and curvature. Correlation analyses between gender and diffusion measures yield different results when volume is included as a covariate. This indicates that incorporating these PVE-related factors in DTI analyses is imperative to disentangle changes in "true microstructural" tissue properties from these hidden covariates.

Introduction

Diffusion tensor imaging (DTI) is a non-invasive imaging technique that can provide information about brain microstructure and the directional organization of neural fiber tissue *in vivo* by measuring the self-diffusion of water molecules (Basser et al., 1994). In brain white matter (WM), diffusion of water is less hindered along than perpendicular to axons, making the local diffusion dependent on local microstructure (Beaulieu, 2002). DTI was first used clinically in schizophrenia (Buchsbaum et al., 1998) and leukoaraiosis (Jones et al., 1999b), where regional changes in diffusion anisotropy or trace were observed in patients but not in healthy controls. These diffusion changes suggest a structural change, which could be detected more easily on DTI scans than on conventional MR images. Since then, the use of DTI in both fundamental research and clinical studies has exploded, with almost a third of all studies on DTI discussing the development of fiber tractography (FT) methods, e.g., Mori et al. (1999), or the use of FT in DTI analyses. FT was initially applied as a method to investigate "brain connectivity" (Basser et al., 2000) and is now often used to increase specificity of observed radiological findings with respect to patient disability, for instance in multiple sclerosis (Wilson et al., 2003; Ciccarelli et al., 2008).

In recent years, DTI and FT have been used extensively to study the microstructural properties of WM fiber pathways. The developing/aging brain, in particular, has been the research topic of many investigations,[1] with studies including subjects ranging from neonates to aging adults. It has been shown repeatedly that the FA of several WM regions (e.g., the cingulum bundles and the uncinate fasciculi) increases during maturation and subsequently decreases with age above the age of approximately 30 years (Bastin et al., 2010; Hasan et al., 2009; Hsu et al., 2008,

* Corresponding author. Image Sciences Institute, University Medical Center Utrecht, Utrecht-3584 CX, The Netherlands.
E-mail address: sjoerd@isi.uu.nl (S.B. Vos).
URL: http://www.isi.uu.nl/ (S.B. Vos).

[1] 57 publications on "DTI brain aging" and 84 on "DTI brain development" since 2009 alone, according to Pubmed.

1053-8119/$ – see front matter © 2011 Elsevier Inc. All rights reserved.
doi:10.1016/j.neuroimage.2011.01.048

2010; Jones et al., 2006; Lebel et al., 2008, in press; Sala et al., in press, 2005; Voineskos et al., 2010, in press). Most of these studies also show an inverse relationship (decrease followed by increase) for the mean diffusivity (MD) and link these diffusion changes to differences in microstructural organization within the WM (Dubois et al., 2008; Lebel et al., 2008). More specifically, changes in radial diffusivity (RD, diffusivity perpendicular to the predominant diffusion direction) and axial diffusivity (AD, diffusivity along the predominant diffusion direction) are believed to reflect different microstructural processes in the WM (Pierpaoli et al., 2001; Song et al., 2002, 2003).

A particular aspect that is known to affect the accuracy of estimated DTI metrics – but which is not always considered a potential cause for correlations or differences in quantitative diffusion analyses – is the partial volume effect (PVE). Reflecting the intra-voxel heterogeneity of different tissue organizations (Alexander et al., 2001; Frank, 2001; Oouchi et al., 2007), Alexander et al. (2001) mentioned that *"the PVE could cause diffusion-based characterization of cerebral ischemia and white matter connectivity to be incorrect"*. Pfefferbaum and Sullivan (2003) have shown that the PVE is also present in the calculation of diffusion measures when averaging data values over regions of interest (ROIs). WM segmentation and semi-automated ROI delineation were used to outline the genu and splenium of the corpus callosum (CC), yielding increased MD values compared to the MD at the center of the WM bundles. This indicates a contamination of the outer WM voxels with its surrounding tissue, which, for the midsagittal genu and splenium of the CC, consists mostly of cerebrospinal fluid (CSF). Several options to mitigate such a CSF contamination have been proposed, such as CSF suppression using fluid-attenuated inversion recovery (FLAIR) acquisition sequences (Papadakis et al., 2002; Cheng et al., in Press), or using a two-tensor model (Pierpaoli and Jones, 2004; Pasternak et al., 2009) to remove the CSF contamination during tensor estimation. However, most DTI studies use neither of these techniques, which leave PVEs with CSF a relevant issue. As partial voluming is not only between WM bundles and CSF, but also, for instance, between different WM bundles, investigations into the effects of the PVE are important to improve quantitative diffusion analyses.

There are several confounding factors related to the PVE that may affect DTI metrics indirectly. For instance, as total WM volume changes with age, and therefore the thickness of some fiber bundles, the relative contribution of PVE-contaminated voxels will be different between bundles of different size (thicker bundles will have a lower contribution of PVE voxels to the entire bundle than thinner bundles), which may introduce a bias in the estimated measures (see Fig. 1 for a schematic example). Not only is bundle volume potentially a hidden covariate in the analysis of DTI metrics, but the orientation and curvature of a bundle may also alter the PVE and thus the diffusion measures.

In this work, we hypothesize that hidden covariates, such as bundle thickness (in the following also referred to as "volume", assuming a constant bundle length and cross-sectional shape), orientation, curvature, and shape modulate the PVE intrinsically and, subsequently, affect the estimated DTI metrics. Previous studies show support for this hypothesis. For instance, investigations of brain volume changes with age show a decline in total WM volume from around the age of 30 (Courchesne et al., 2000; Liu et al., 2003; Resnick et al., 2003), matching the age-FA relation mentioned previously. Another study shows a left-sided co-lateralization of FA and concomitant bundle volume, potentially indicative of a more general agreement between morphometry and diffusion properties (Huster et al., 2009).

Using simulations of synthetic diffusion phantoms (Leemans et al., 2005) we determine whether the PVE-related covariates (volume, orientation, and curvature) affect the estimated diffusion measures. With these simulations, it is possible to change the volume, orientation, or curvature of a bundle independently while keeping all other configurational properties fixed. This allows for investigations of only the specific covariate of interest in relation to the estimated DTI metrics. In addition, the cingulum bundles and the CC of 55 healthy subjects are reconstructed using FT to examine whether the PVE-related confounding factors are present in experimental DTI

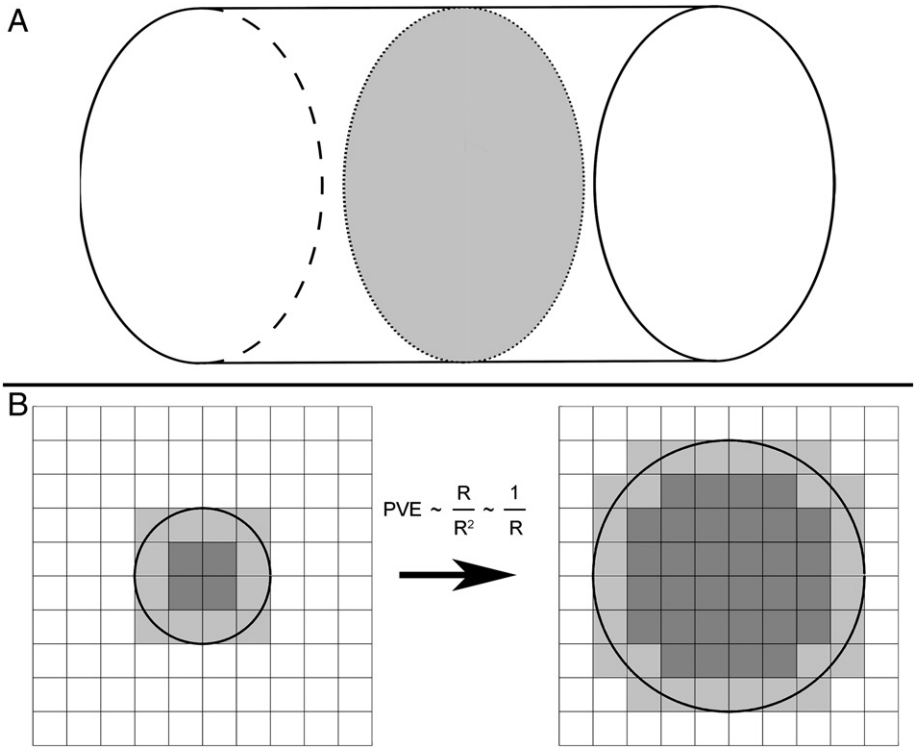

Fig. 1. Schematic representation of the partial volume effect (PVE) in a 3D object. The PVE is defined as the volume-to-surface ratio of an object. For a cylinder, which has a circular cross-section (indicated as the shaded area in A), this can be simplified to a circle, which has a surface-to-circumference ratio. Further simplification yield that the PVE scales with $1/R$ (with R the radius of the circle), showing that increasing volume means a reduction in PVE. This is shown in B, where a small and big circle have been plotted on a square grid. The relative number of PVE voxels (light gray) compared to voxels enclosed completely by the circle (dark gray) is larger for a small circle (left) than for a big circle (right).

data. The interest by many researchers in these bundles has resulted in an abundance of information about diffusion changes, and thus valuable reference material for this study (Davis et al., 2009; Huster et al., 2009; Jones et al., 2006; Lebel et al., 2008; Malykhin et al., 2008; Salat et al., 2005). The cingulum does not interface with CSF-filled spaces, in contrast with the CC, which is partially adjacent to the lateral ventricles and the longitudinal fissure. In regions where there is proximity to the ventricles, for example, one observes "spikes" in the MD values (Jones et al., 2005). The large difference in the surrounding tissues makes these bundles ideal candidates to determine the potential effect of PVE-related covariates on the different diffusion parameters. By investigating correlations between the volume of the bundles and specific diffusion properties of these bundles, the presence of such a hidden covariate may be revealed.

Our results demonstrate that DTI metrics are indeed correlated with volume, orientation, and curvature of a fiber bundle. As such, several conclusions drawn from previous analyses – aging studies in particular – should be nuanced in the light of these PVE-related covariates in order to correctly classify whether the observed changes in diffusion measures originate from either changes in macrostructural/morphological or microstructural properties, or a combination of both. Observed relations between age and diffusion properties are altered by the inclusion of volume as a covariate, which indicates that it is required to include this confound in quantitative analyses. Preliminary results of this work on PVE-related covariates have been presented at the 2010 Joint ISMRM–ESMRMB meeting in Stockholm, Sweden (Vos et al., 2010).

Materials and methods

Fiber bundle simulations

Simulations of neural fiber bundles were performed according to Leemans et al. (2005) to investigate the following potentially confounding factors in FT-based analyses: (i) fiber bundle thickness (predefined range: 9–13 mm); (ii) pathway orientation (in-plane rotation range: 0–15°); and (iii) bundle curvature (inverse radius range: 0.035–0.055 mm^{-1}). Keeping all other simulation parameters unchanged, only the contribution of PVE-contaminated voxels to the bundles differs between the simulations. The effect of these factors was examined using FA = 0.9 and MD = 0.0007 mm^2/s within the bundle, and two different bundle environments: one representing the CC segment environment (in the following referred to as "CC simulations", with background FA = 0 and MD = 0.0032 mm^2/s); and one representing the cingulum environment (in the following referred to as "cingulum simulations", with background FA and MD values equal to the values within the fiber bundle, albeit with a different orientation) (Le Bihan et al., 2001; Jones and Basser, 2004). In total, six sets of simulations were performed (Fig. 2). Fiber bundles were simulated with 2 mm isotropic voxel size and a Gaussian profile across the bundle. For more detailed information on the simulation framework, the reader is referred to (Leemans et al., 2005). Deterministic FT (Basser et al., 2000) was performed in *ExploreDTI* (Leemans et al., 2009) with an FA tracking threshold of 0.2 and an angle threshold of 30°.

Data acquisition

Cardiac-gated DTI data were acquired from 55 healthy volunteers (37 females and 18 males), aged 18.4 to 44 years (median age 31.9 years), on a 3T system using a single-shot spin-echo EPI sequence with a b-value of 1200 s/mm^2 along 60 directions (Jones et al., 1999a), with 6 B0-images and ASSET factor = 2. The acquisition matrix of 96 × 96 was reconstructed to 128 × 128 with a field-of-view of 230 × 230 mm^2 and 60 axial slices with thickness 2.4 mm were acquired without gap. This resulted in an effective TR of 15 R–R intervals and a total acquisition time of approximately 25 min. All subjects gave a written informed consent to participate in this study under a protocol approved by the Cardiff University Ethics Committee.

Image processing

Prior to data analysis, the acquired images were corrected for eddy current induced geometric distortions and subject motion by realigning all diffusion-weighted images (DWIs) to the B0-images

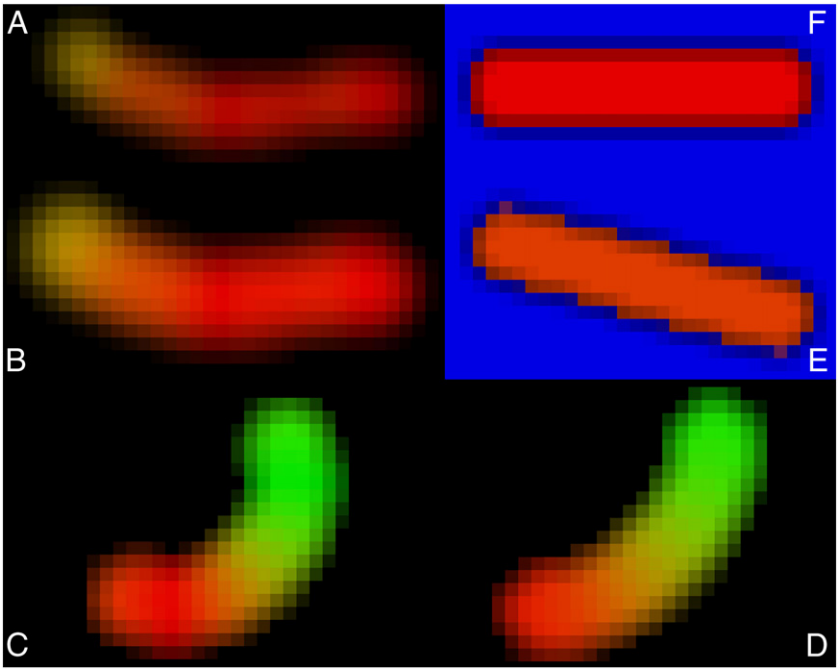

Fig. 2. Simulated fiber bundles of varying thickness (A and B), curvature (C and D), and orientation (E and F). A–D are examples of cingulum simulations, with a fiber bundle in an isotropic surrounding with high diffusivity; whereas E–F are examples of CC simulations, with an anisotropic environment oriented perpendicularly to the simulated bundles.

(non-diffusion weighted images) with elastix (Klein et al., 2010) using an affine coregistration technique (12 degrees of freedom) with mutual information as the cost function (Pluim et al., 2003). In this procedure, the diffusion gradients were adjusted with the proper b-matrix-rotation as described by Leemans and Jones (2009). The diffusion tensor model was fitted using the Levenberg–Marquardt nonlinear regression method (Marquardt, 1963), initiated with the fitted values from a weighted linear least squares estimation. All DTI scans were rigidly transformed to MNI space in the motion–distortion correction procedure (Rohde et al., 2004).

Tractography

To determine whether PVE-related confounds affect FT-based analyses of DTI metrics in experimental data we investigated the characteristics of the cingulum and the CC. Whole brain FT parameters were identical to the ones used for the simulated diffusion data. To investigate the existence of the aforementioned covariates when analyzing diffusion measures of the cingulum bundle, a specific segment was selected in the dorsal part of the cingulum. The segments were defined by placing three "AND" ROIs at selected anatomical landmarks (Emsell et al., 2009) and placing two ROIs 10 mm anterior (S1) and posterior (S2) of the central "AND" ROI (Fig. 3). Only the tract segment, i.e., the part of the fiber bundle between ROIs S1 and S2, was investigated. In doing so, there were no intersubject differences in segment length, which ensures consistency in estimating the volume of the fiber bundles. Bundle characteristics were calculated by averaging diffusion measures for all voxels intersected by that bundle, with each voxel only counted once (Concha et al., 2005a,b, 2009; Eluvathingal et al., 2007; Lebel et al., in press), and defining segment volume as the total volume of the voxels intersected by that bundle. ROIs were defined by a single blinded rater.

The second bundle that was studied was the CC. Only the medial part of the CC, which is (almost) entirely surrounded by CSF, was investigated to test whether the influence of the PVE on DTI measures may be different from bundle configurations where the fiber bundles are surrounded by other WM structures and not by CSF. Segments of 4 mm length to either side of the midsagittal slice were selected (Fig. 4): a length that is long enough to have a large spread in segment volumes, but short enough so that the segment is still surrounded by CSF only. As all data were analyzed in MNI space, the midsagittal slice could be determined reliably in all subjects.

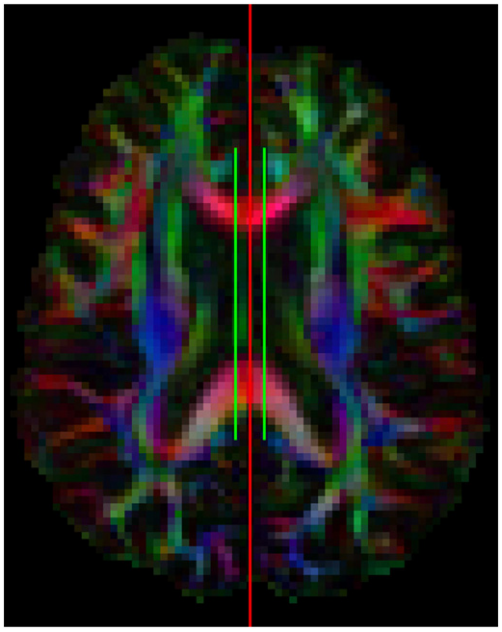

Fig. 4. Selection of the medial segment of the corpus callosum. The red line represents the midsagittal plane in MNI space, and the two segment-selecting regions-of-interest (green) are drawn two voxels (4 mm) to either side of the midsagittal plane.

Statistical evaluation

To test the hypothesis that bundle volume is a PVE-related covariate, Spearman's rank correlation coefficients between DTI metrics (FA, MD, AD, and RD) and segment volume were calculated. According to our hypothesis, segment volume should be added as a covariate not-of-interest in further analyses, for instance, when calculating the correlation between age and bundle-specific quantitative measures. Using multiple regression we have tested whether there was a significant linear or quadratic relation between age and diffusion measures (Hsu et al., 2010), and whether the inclusion of volume as a covariate yielded a different outcome in these analyses.

Previously, diffusion values of the cingulum were found to differ between males and females and between the left and the right bundle (Huster et al., 2009). Segment volume was incorporated into these analyses as a covariate, to examine whether any observed differences

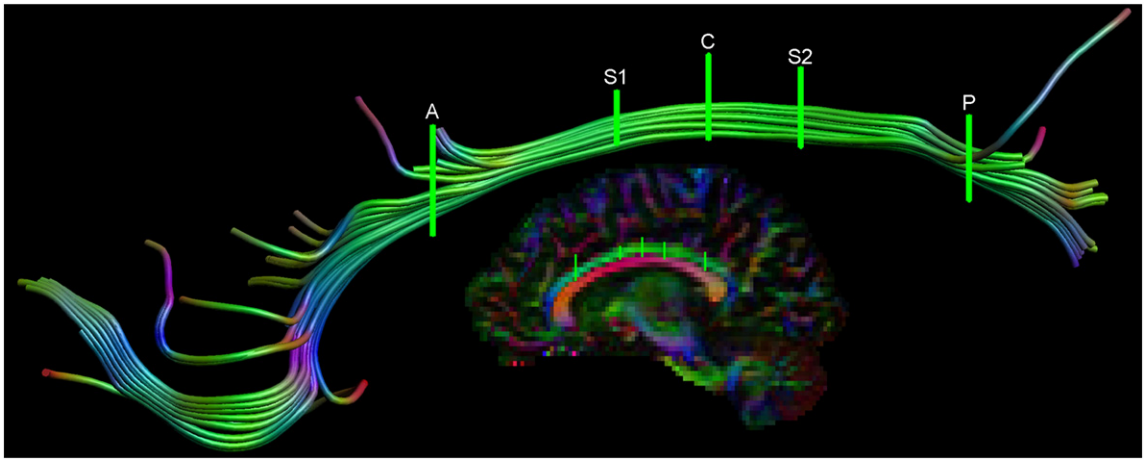

Fig. 3. Selection of the cingulum segment. Anterior (A) and posterior (P) regions of interest (ROI) were placed at the most posterior slice showing the genu in full profile and the most anterior slice showing the splenium in full profile, respectively. Central (C) ROI was placed at midpoint between A and P, with segment-selecting ROIs placed five voxels (10 mm) anterior (S1) and posterior (S2) of C.

in diffusion measures between left and right cingulum bundles or between males and females were due to volume differences.

Results

PVE-related covariates in simulations

All six sets of simulations (changes in volume, orientation, and curvature, for both the cingulum and CC simulations) showed a clear effect of these PVE-related covariates on the estimated DTI metrics. Bundle volume demonstrated a monotonous relation with the diffusion measures (Fig. 5). By contrast, the other PVE-modulating factors generally displayed a high degree of non-monotonicity (Figs. 6 and 7).

Experimental data

Correlations between segment volume and DTI metrics have been visualized in Fig. 8 for the cingulum and in Fig. 9 for the CC. A positive correlation of FA with volume ($p = 0.028$) was found for the cingulum segments, and the CC segments showed a significant decrease of MD with segment volume ($p = 0.0039$). To reveal the underlying causes for these correlations, subsequent analyses were performed to determine whether AD and/or RD were correlated with segment volume. In the cingulum, a downward trend of RD with segment volume was observed (Fig. 8). In the CC, the correlation between MD and volume was due to underlying decreases of both AD and RD with segment volume ($p = 0.021$ and $p = 0.0037$, respectively) (Fig. 9).

Investigation of the effect of age on bundle-specific quantitative measures demonstrated that in the CC segment only the FA correlated significantly (decreasing linearly) with age ($p = 0.0056$). Inclusion of bundle volume as a covariate did not alter this relation. For the cingulum, no significant relation with age was observed, with or without including volume as a covariate.

No gender-related differences in diffusivity measures were observed for the cingulum. For the CC, including volume as a covariate yielded a significantly higher FA and lower MD, caused by a significantly lower RD, in females than in males. These effects could not be observed without segment volume as a covariate (Table 1).

Intrasubject analysis of left and right cingulum segments revealed a significantly higher AD left than right, with or without segment volume as a covariate. There was no significant difference in the corresponding FA, MD, or RD values between the left and the right cingulum segments (Table 2).

Discussion

Several factors, e.g., bundle thickness, orientation, and curvature may change the PVE and thus the analysis and estimation of bundle-averaged DTI metrics. These PVEs originate from the acquisition: signal averaging over finite-size voxels may include more than one structure. As already illustrated in Fig. 1, bundles can be influenced differently by the PVE depending on bundle thickness. However, a single bundle may also be affected by its position relative to the acquisition matrix. Consider the simulated fiber bundle shown in Fig. 10A(i), which is perfectly aligned with the voxel grid. If the bundle is not perfectly aligned with the acquisition grid (Fig. 10A (ii)–(iv)), the outer voxels are PVE voxels, which affect the estimated DTI metrics of the bundle, as seen in Fig. 10B. Such a "gridding effect" affects the reproducibility of DTI analyses negatively. Therefore, it is important to tease out possible covariates that may confound the estimation of diffusion measures in order to improve the reliability of DTI analyses.

Proof of principle

Previously, it has been shown that CSF contamination in PVE voxels influences voxel-wise DTI metrics (Papadakis et al., 2002; Chou et al., 2005). In this work, however, we investigated whether PVE modulating factors (i.e., bundle volume, orientation, and curvature) cause significant differences in diffusion measures of large, multi-voxel regions. To highlight this issue for experimental data, we also

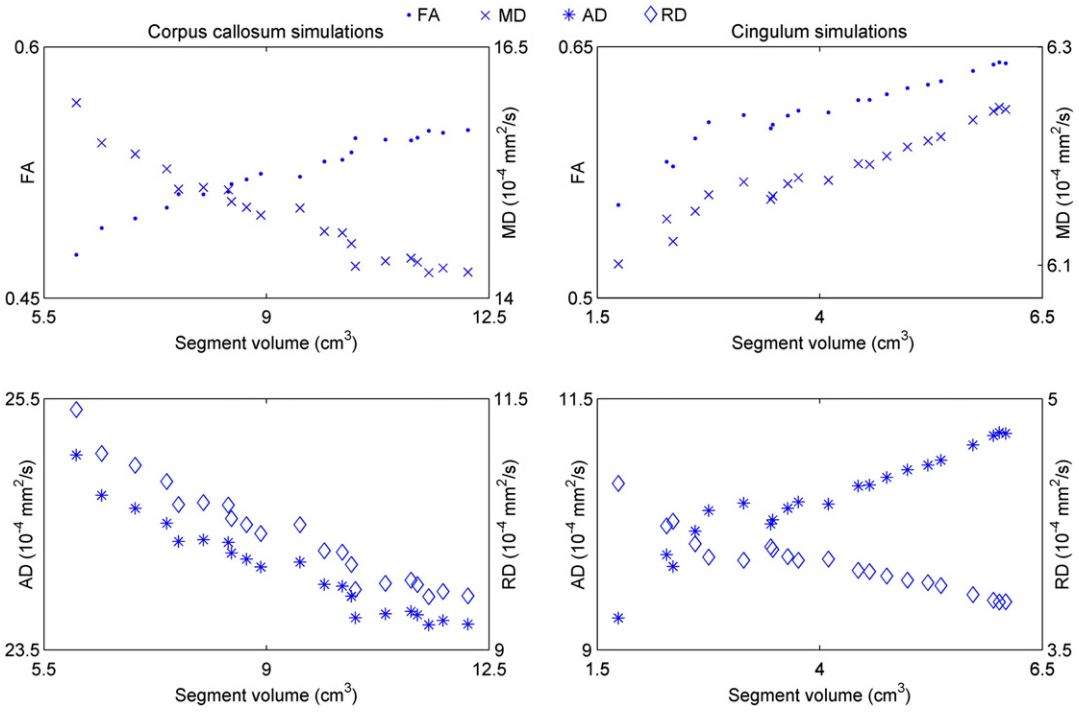

Fig. 5. Dependence of DTI metrics on bundle volume. The plots in the left column show the results of the corpus callosum (CC) simulations; plots in the right column show the results of the cingulum simulations. These plots show that bundle volume modulates, through the PVE, all estimated diffusion parameters: FA, MD, axial diffusivity (AD), and radial diffusivity (RD).

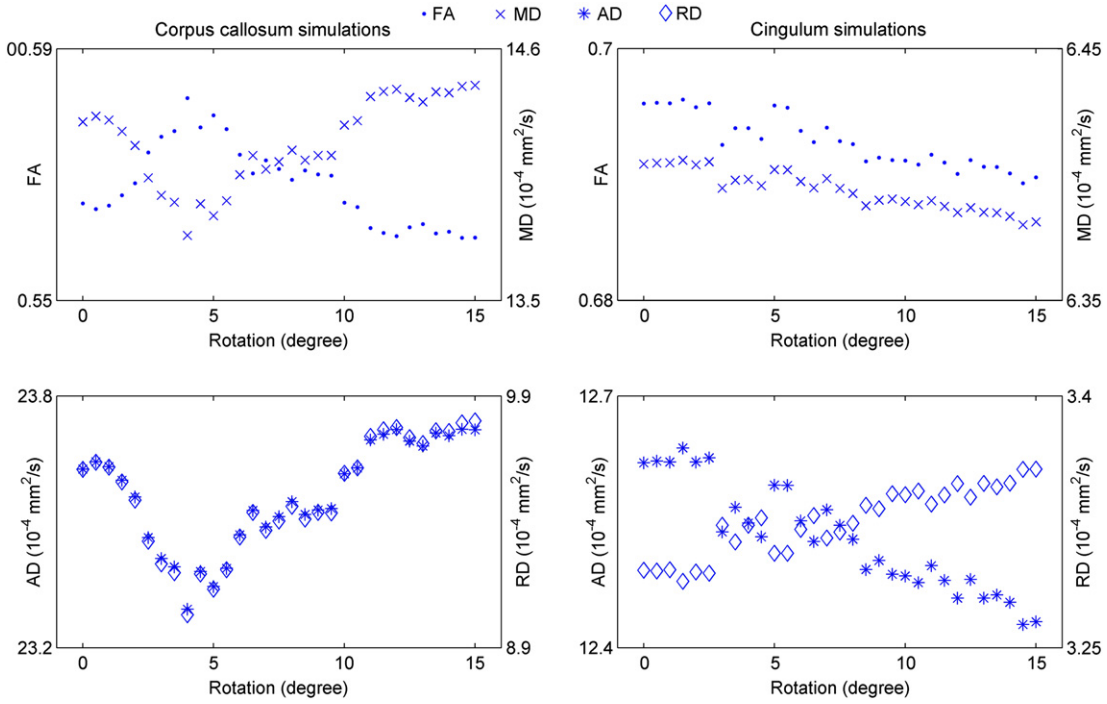

Fig. 6. Dependence of DTI metrics on bundle orientation. The plots in the left column show the results of the corpus callosum (CC) simulations; plots in the right column show the results of the cingulum simulations. In these simulations, the simulated bundle is rotated over a range of 15°, and the resulting effect of orientation can be seen in all DTI measures (FA; MD; axial diffusivity, AD; and radial diffusivity, RD). The non-linear dependence of diffusion metrics on the investigated confounds shows that these effects are non-trivial.

performed an analysis in which volume can be considered as the only PVE modulating factor. More specifically, we examined the existence of a relation between DTI parameters of the CSF and the total CSF volume. The diffusivity of CSF should be roughly the same across individuals, so no correlation with volume is expected. However, as the MD of PVE voxels is decreased compared to non-PVE voxels of the CSF (Chou et al., 2005), one can expect that for smaller CSF volumes (where the relative contribution of PVE voxels is higher than for larger CSF volumes) the estimated MD would be lower. This relation is confirmed by segmenting all CSF voxels using an automated gray-level thresholding method, performed on the MD map (Otsu, 1979), and correlating the total volume of CSF with the estimated DTI metrics

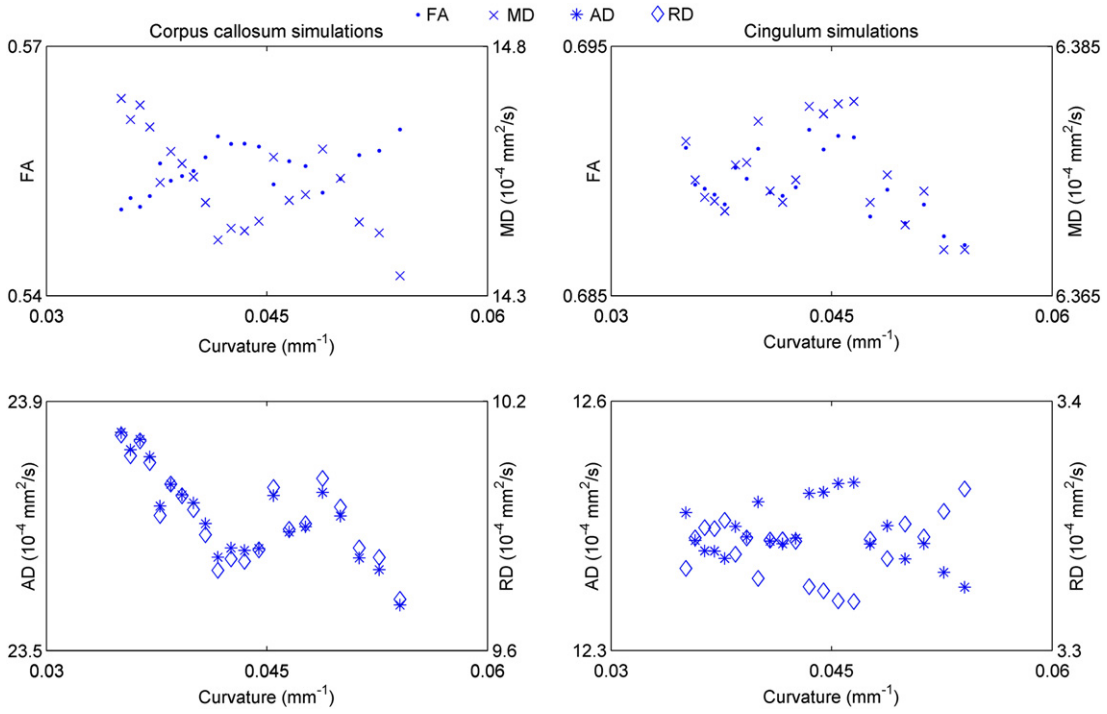

Fig. 7. Dependence of DTI metrics on bundle curvature. The plots in the left column show the results of the corpus callosum (CC) simulations; plots in the right column show the results of the cingulum simulations. In these simulations, the curvature of the simulated bundle is increased, causing a change in FA and MD through a change in axial and radial diffusivity (AD and RD, respectively). The non-linear dependence of DTI metrics on the investigated confounds shows that these effects are non-trivial.

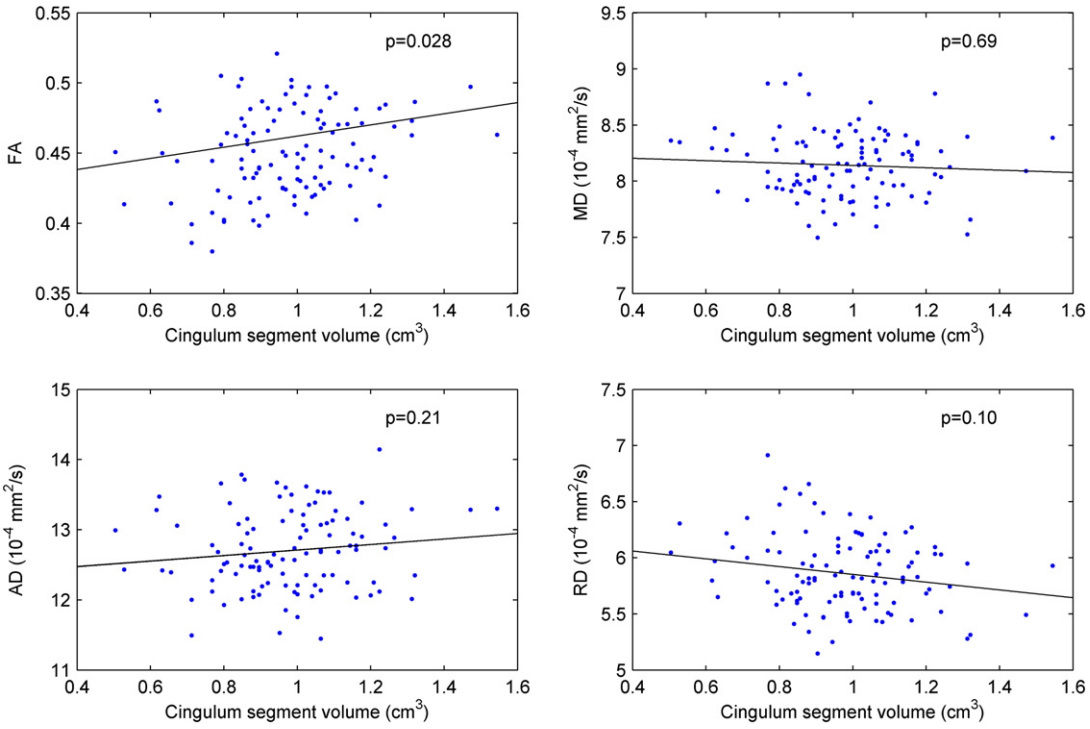

Fig. 8. Correlation of DTI metrics and volume for the cingulum segments. A significant increase in fractional anisotropy (FA) with volume is observed, whereas no significant changes in mean, axial, or radial diffusivity are observed (MD, RD, and AD, respectively). The increase in FA is caused by opposite trends of AD and RD with volume. While non-parametric tests have been used to test for correlations, parametric tests have been used for the plotted lines to show the trends in the data.

in that volume. The FA decreases with larger CSF volumes, whereas the MD, AD, and RD show a distinct positive correlation with CSF volume. This proof of concept clearly demonstrates the existence of a confounding factor (in this case the volume of CSF regions) that affects the PVE contribution and, in turn, the estimation of DTI measures.

PVE-related covariates in simulations

The effect of PVE modulation can be observed in both the cingulum and the CC simulations, where bundle volume and FA are strongly correlated ($p<0.001$). The induced change in FA is caused by a

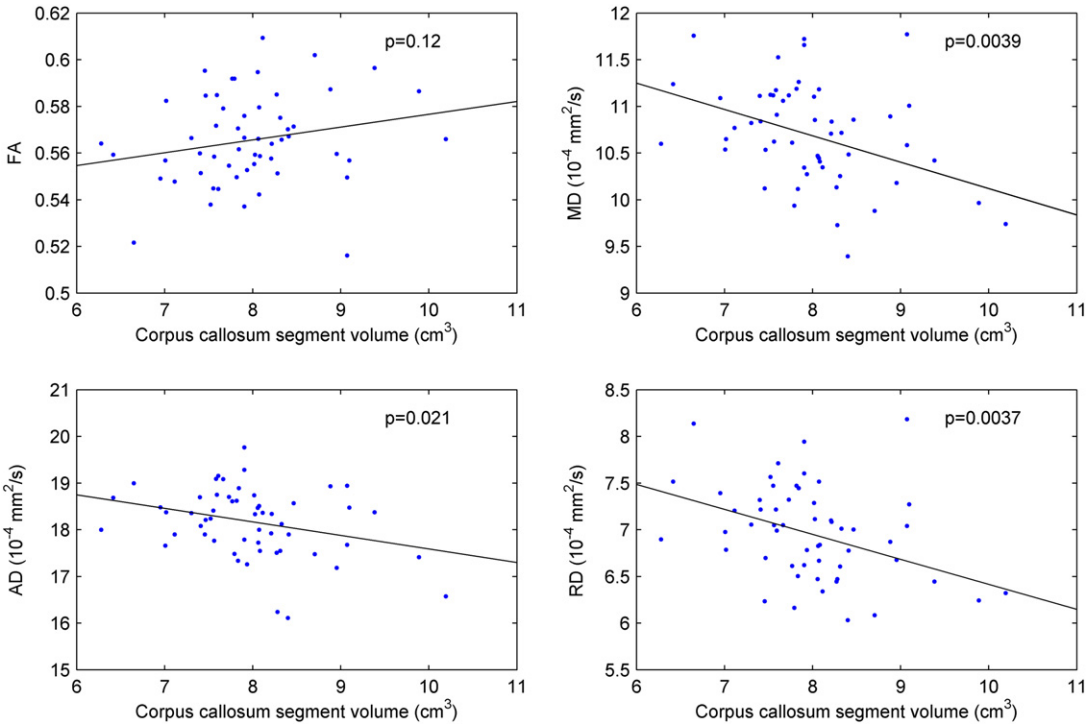

Fig. 9. Correlation of DTI metrics and volume for the corpus callosum (CC) segments. No significant change in fractional anisotropy (FA) with volume is observed, whereas the mean diffusivity (MD) decreased significantly with volume. The decrease in MD is caused by negative correlations of axial and radial diffusivity (AD and RD, respectively) with segment volume. While non-parametric tests have been used to test for correlations, parametric tests have been used for the plotted lines to show the trends in the data.

Table 1
Gender comparison of bundle segments.

		Female	Male
Cingulum segment	Volume (cm^3)	0.942 ± 0.166	$1.045 \pm 0.195^{*}$
	Fractional anisotropy	0.448 ± 0.032	0.456 ± 0.028
	MD[a] (10^{-4} mm^2/s)	8.16 ± 0.26	8.12 ± 0.36
Corpus callosum segment	Volume (cm^3)	7.857 ± 0.787	8.215 ± 0.665
	Fractional anisotropy	0.569 ± 0.019	$0.559 \pm 0.019^{\dagger}$
	MD[a] (10^{-4} mm^2/s)	10.63 ± 0.55	$10.86 \pm 0.47^{\dagger}$

[a] Mean diffusivity.
* $p<0.01$ not including volume as covariate.
† $p<0.05$ including volume as covariate.

significant reduction in RD in both sets of simulations, a decrease of AD in the CC simulations, and an increase of AD in the cingulum simulations (Fig. 5). In all simulations, the relative changes in RD were larger than or equal to the relative changes in AD, showing that changes in RD are the main underlying cause of the observed changes in FA. These results indicate that the contribution of PVE-contaminated voxels reduces with increased volume and that this PVE-related covariate influences the analysis of diffusion parameters. In these simulations, a constant cross-sectional shape has been defined. It is important to note that for bundles with a more irregular shape, larger volumes do not necessarily result in a higher PVE-contamination.

A relation was also observed between DTI metrics and two other confounds, i.e., orientation and curvature, but not all simulations showed a monotonous relation (Figs. 6 and 7). These changes, especially in the CC simulations, demonstrate that the effects of orientation and curvature are non-trivial. Although the simulations showed a strong effect of PVE altering factors on diffusion measures, in particular for volume, these results can only be regarded as an approximation: in each set of simulations only one factor was varied, whereas real data will show variation in volume, orientation, and curvature between different (parts of) bundles simultaneously.

Experimental data

The effect of bundle volume on diffusion measures in the simulations was larger than the effects of curvature and orientation. We have therefore focussed only on bundle volume as a potential PVE-modulating covariate in the experimental DTI data.

Group analysis of the cingulum bundles showed a positive correlation between the volume of the cingulum segment and FA (Fig. 8). Adjacent WM-bundles have a high diffusivity perpendicular to the cingulum and low diffusivity parallel to the cingulum, and the PVE, therefore, is expected to affect both AD and RD. In the cingulum segments, however, this has not lead to significance relations with volume. Thanks to the opposite trends of AD and RD with volume, the FA increased and the MD was unchanged. These findings are in agreement with the known fact that the MD does not depend on PVE changes in the cingulum bundle, inasmuch as it is surrounded by gray matter and other WM structures, both of which have similar MD values in the Gaussian b-value regime (Pierpaoli et al., 1996; Yoshiura et al., 2001).

For the cingulum simulations (Fig. 5), the average MD within the bundle was affected by the hidden covariates. However, the changes were relatively small compared to the absolute values. Although these findings could not be observed in the experimental data, detecting such small changes in MD values in acquired DTI data is harder than in simulations because of noise and natural variability between subjects. Furthermore, there is more than one PVE modulating covariate affecting the diffusion metrics in experimental data, whereas only one factor was changed in the simulations. Overall, the results observed in the simulations are in very good agreement with the experimental findings of the cingulum segments.

In structures adjacent to CSF, for instance the CC, one would expect changes in PVE to affect the MD as well. CSF should exhibit unhindered diffusion and hence a high MD, so, in theory, PVE contamination with CSF will increase the estimated MD of the CC bundle (similar to the proof of concept analysis). This means that a thinner CC would have a higher MD than a thicker CC. In the group analysis of the medial part of the CC, a significant decrease of MD with increasing bundle volume was observed, showing that the MD depended on PVE-related changes due to bundle thickness (Fig. 9). Although the MD decreased significantly, caused by a decrease in both its axial and its radial component, only an upward trend of FA with volume was observed. Here, the inter-subject variability in terms of local curvature and orientation, or true microstructural differences (e.g., axon diameter or axon packing density) may be too large to infer a clear FA relationship.

The observed changes in MD are in accordance with previously reported measurements, showing significant increases from adolescents to older adults (mean age 18.9 years and 67.6 years, respectively) in structures adjacent to CSF (e.g., the genu of the CC and the fornix), whereas deep WM (e.g., pericallosal) areas showed no change (Bennett et al., 2010). Next to "microstructural" changes, these differences in MD between adolescents and older adults may be explained in part on the basis of WM atrophy, i.e., WM tissue loss due to aging. Shrinkage of the WM causes thinning of several fiber bundles and, as we have shown in this work for the CC, the MD depends on the thickness of this fiber bundle. Although changes in diffusion measures are observed even when correcting for volume (Bendlin et al., 2010), atrophy could still explain part of the observed variance of diffusion measures with age.

As shown in this work, bundle volume is significantly correlated with bundle-specific quantitative measures, and should therefore be included as a covariate in the analysis of age on these measures. Independent of whether segment volume has been included as a covariate, we showed a linear decrease of FA with age for the CC segment. The diffusion measures for the cingulum, and the MD, AD, and RD for the CC showed no significant age relation. This is due to the age range of the subjects, which is located at the peak of the quadratic relation between age and DTI measures (Hsu et al., 2010). In studies where an age effect has been demonstrated, such as Lebel et al. (2008) and Hsu et al. (2010), the importance of WM volume as a covariate in DTI analyses is even more essential to specify whether the cause of the observed age effects is due to changes in bundle volume, "true microstructural" change, or both.

In the investigation of differences in diffusion measures between genders, incorporating volume into the analysis yielded a significant difference in the FA, MD, and RD of the CC. A higher FA and lower MD were observed in females than in males, originating from significantly lower RD values in males. These differences were only observed when volume was incorporated in the analysis 1, showing that including volume as a covariate is imperative.

Besides the "gridding effect" due to discrete sampling, preprocessing of the DWIs (e.g., motion correction) introduces additional PVE.

Table 2
Intrasubject comparison of cingulum bundle segments.

	Left	Right
Segment volume (cm^3)	0.031 ± 0.167	$0.921 \pm 0.181^{*}$
Fractional anisotropy	0.456 ± 0.031	0.445 ± 0.029
MD[a] (10^{-4} mm^2/s)	8.11 ± 0.29	8.12 ± 0.29
AD[b] (10^{-4} mm^2/s)	12.84 ± 0.54	$12.57 \pm 0.54^{*,\dagger}$
RD[c] (10^{-4} mm^2/s)	5.84 ± 0.34	5.90 ± 0.32

[a] Mean diffusivity.
[b] Axial diffusivity.
[c] Radial diffusivity.
* $p<0.01$ not including volume as covariate.
† $p<0.05$ including volume as covariate.

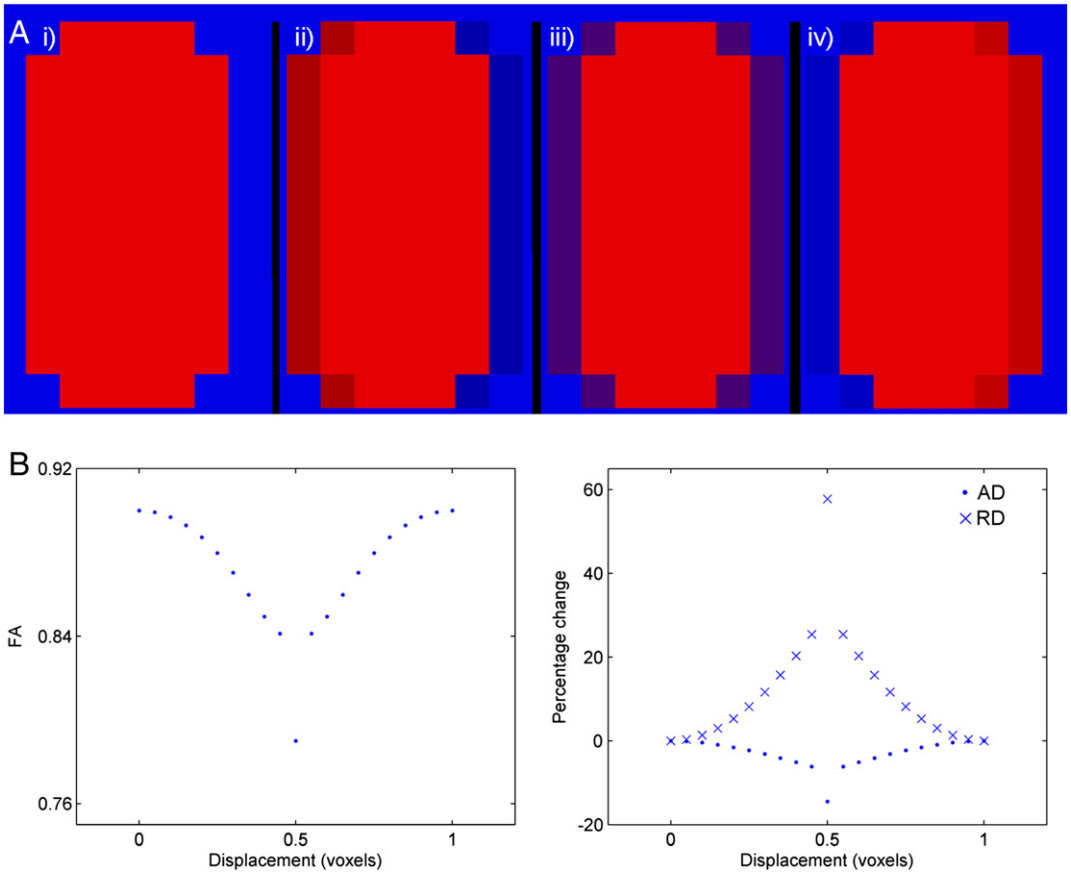

Fig. 10. The relative position of a simulated fiber bundle on the voxel grid changes the partial volume effect (PVE). In this simulation, the background has a high fractional anisotropy (FA) and orientation perpendicular to the bundle. A (i) shows a simulated bundle aligned with the voxel grid, (ii)–(iv) show the bundle misaligned by 0.3, 0.5, and 0.8 voxels horizontally, respectively. B shows the DTI metrics as a function of relative position to the voxel grid (FA; mean diffusivity, MD: axial diffusivity, AD; radial diffusivity, RD). The resulting differences in PVE of these bundles (as can be seen in A) lead to changes in the estimated DTI metrics.

The preprocessing steps, as well as the extent of the corrected motion and distortions, are roughly equal for all subjects. This means that the intersubject variability in volume and diffusion estimates subjects may be increased, but any underlying trends will not be altered.

An FA threshold of 0.2 and an angle threshold of 30° have been used to reconstruct the fiber pathways. Although these values are often used in deterministic FT, there are also many studies using a less strict threshold, such as FA thresholds of 0.15 or 0.1. One can imagine that if such more liberal thresholds are used, FT will include more voxels on the edges of bundles, thereby increasing the PVE contribution to the bundle. A clear example of this has been shown in the work of Taoka et al. (2009), where the uncinate fasciculus (UF) has been tracked with four different FA tracking thresholds (0.1, 0.15, 0.2, and 0.25). As a result of changing this FT parameter, they found an increase in UF volume, accompanied by lower FA and higher MD values in the UF, when using lower FA thresholds. The inclusion of more PVE voxels with lower thresholds increased the bundle volume, and consequently modulated the estimated FA and MD values. We have chosen to use strict tracking parameters to show that even when using conservative parameters, the PVE-related confounds still affect the DTI metrics.

Implications and future work

The results presented in this work are not limited to FT-based analyses. Since bundle thickness is inherently an underlying factor, ROI-based (Mukherjee et al., 2001; Bonekamp et al., 2007), voxel-based (Madden et al., 2009; Westlye et al., 2009), and atlas-based analyses (Huang et al., 2006; Fjell et al., 2008) suffer from these confounds as well. Similarly, these effects are not limited to the tensor framework, but also apply to other approaches of diffusion modeling, such as spherical deconvolution and Q-ball imaging (Tournier et al., 2004; Tuch, 2004), among others. To truly examine the extent of PVE-related confounds in diffusion analyses, future studies should aim to clarify the effect sizes of different factors influencing diffusion measures.

Being cross-sectional by design, this study cannot uncouple potentially true microstructural changes from morphological confounds, such as bundle volume, orientation, or curvature, across different subjects. Longitudinal studies could overcome this drawback by comparing bundle volume and configuration over time as well as age and DTI parameters. For instance, if in such a study covariates not-of-interest remain unchanged but diffusion measures do change, those changes truly reflect changes in microstructure. Given a sufficient total follow-up time and regular examination of bundle characteristics, such studies should be able to determine the effects of these factors on the estimated diffusion metrics, and during what stage of development and/or aging these changes occur.

In conclusion, our work shows that bundle volume, orientation, and curvature are PVE-modulating factors that, subsequently, affect the estimation of diffusion metrics when sampled along the tract. These findings further our understanding of causality when interpreting the results of DTI analyses. In other words, we have shown the existence of variables that have not been considered previously, volume in particular, contributing to the explanation of the observed differences in DTI measures between populations (e.g., males *vs.* females). To disentangle "true microstructural" from macrostructural and configurational differences/relations or, more generally, to

improve the specificity of quantitative DTI analyses, we suggest to include volume as a covariate not-of-interest in future studies.

Acknowledgments

This work was financially supported by the Care4Me (Cooperative Advanced REsearch for Medical Efficiency) pan-European research program ITEA (Information Technology for European Advancement). The authors would like to thank Dr. John Evans, Chief Physicist of CUBRIC, for assistance in acquiring the MR data.

References

Alexander, A.L., Hasan, K.M., Lazar, M., Tsuruda, J.S., Parker, D.L., 2001. Analysis of partial volume effects in diffusion-tensor MRI. Magn. Reson. Med. 45 (5), 770–780.
Basser, P.J., Mattiello, J., LeBihan, D., 1994. MR diffusion tensor spectroscopy and imaging. Biophys. J. 66 (1), 259–267 Jan.
Basser, P.J., Pajevic, S., Pierpaoli, C., Duda, J., Aldroubi, A., 2000. In vivo fiber tractography using DT-MRI data. Magn. Reson. Med. 44 (4), 625–632.
Bastin, M.E., Muñoz Maniega, S., Ferguson, K.J., Brown, L.J., Wardlaw, J.M., MacLullich, A.M., Clayden, J.D., 2010. Quantifying the effects of normal ageing on white matter structure using unsupervised tract shape modelling. Neuroimage 51 (1), 1–10.
Beaulieu, C., 2002. The basis of anisotropic water diffusion in the nervous system — a technical review. NMR Biomed. 15 (7–8), 435–455.
Bendlin, B.B., Fitzgerald, M.E., Ries, M.L., Xu, G., Kastman, E.K., Thiel, B.W., Rowley, H.A., Lazar, M., Alexander, A.L., Johnson, S.C., 2010. White matter in aging and cognition: a cross-sectional study of microstructure in adults aged eighteen to eighty-three. Dev. Neuropsychol. 35 (3), 257–277.
Bennett, I.J., Madden, D.J., Vaidya, C.J., Howard, D.V., Howard Jr., J.H., 2010. Age-related differences in multiple measures of white matter integrity: a diffusion tensor imaging study of healthy aging. Hum. Brain Mapp. 31 (3), 378–390.
Bonekamp, D., Nagae, L.M., Degaonkar, M., Matson, M., Abdalla, W.M., Barker, P.B., Mori, S., Horská, A., 2007. Diffusion tensor imaging in children and adolescents: reproducibility, hemispheric, and age-related differences. Neuroimage 34 (2), 733–742.
Buchsbaum, M.S., Tang, C.Y., Peled, S., Gudbjartsson, H., Lu, D., Hazlett, E.A., Downhill, J., Haznedar, M., Fallon, J.H., Atlas, S.W., 1998. MRI white matter diffusion anisotropy and PET metabolic rate in schizophrenia. NeuroReport 9 (0959–4965), 425–430 February.
Cheng, Y.-W., Chung, H.-W., Chen, C.-Y., Chou, M.-C., in Press. Diffusion tensor imaging with cerebrospinal fluid suppression and signal-to-noise preservation using acquisition combining fluid-attenuated inversion recovery and conventional imaging: Comparison of fiber tracking. Eur. J. Radiol. doi:10.1016/j.ejrad.2009.12.032.
Chou, M.-C., Lin, Y.-R., Huang, T.-Y., Wang, C.-Y., Chung, H.-W., Juan, C.-J., Chen, C.-Y., 2005. FLAIR diffusion-tensor MR tractography: comparison of fiber tracking with conventional imaging. AJNR Am. J. Neuroradiol. 26 (3), 591–597.
Ciccarelli, O., Catani, M., Johansen-Berg, H., Clark, C., Thompson, A., 2008. Diffusion-based tractography in neurological disorders: concepts, applications, and future developments. Lancet Neurol. 7 (8), 715–727.
Concha, L., Beaulieu, C., Collins, D.L., Gross, D.W., 2009. White-matter diffusion abnormalities in temporal-lobe epilepsy with and without mesial temporal sclerosis. J. Neurol. Neurosurg. Psychiatry 80 (3), 312–319.
Concha, L., Beaulieu, C., Gross, D.W., 2005a. Bilateral limbic diffusion abnormalities in unilateral temporal lobe epilepsy. Ann. Neurol. 57 (2), 188–196.
Concha, L., Gross, D.W., Beaulieu, C., 2005b. Diffusion tensor tractography of the Limbic System. AJNR Am. J. Neuroradiol. 26 (9), 2267–2274.
Courchesne, E., Chisum, H.J., Townsend, J., Cowles, A., Covington, J., Egaas, B., Harwood, M., Hinds, S., Press, G.A., 2000. Normal brain development and aging: quantitative analysis at in vivo MR imaging in healthy volunteers. Radiology 216 (3), 672–682.
Davis, S.W., Dennis, N.A., Buchler, N.G., White, L.E., Madden, D.J., Cabeza, R., 2009. Assessing the effects of age on long white matter tracts using diffusion tensor tractography. Neuroimage 46 (2), 530–541.
Dubois, J., Dehaene-Lambertz, G., Perrin, M., Mangin, J.-F., Cointepas, Y., Duchesnay, E., Le Bihan, D., Hertz-Pannier, L., 2008. Asynchrony of the early maturation of white matter bundles in healthy infants: quantitative landmarks revealed noninvasively by diffusion tensor imaging. Hum. Brain Mapp. 29 (1), 14–27.
Eluvathingal, T.J., Hasan, K.M., Kramer, L., Fletcher, J.M., Ewing-Cobbs, L., 2007. Quantitative diffusion tensor tractography of association and projection fibers in normally developing children and adolescents. Cereb. Cortex 17 (12), 2760–2768.
Emsell, L., Leemans, A., Langan, C., Barker, G., van der Putten, W., McCarthy, P., Skinner, R., McDonald, C., Cannon, D.M., 2009. A DTI tractography study of the cingulum in euthymic bipolar I disorder. Proceedings of the 17th Annual Meeting of International Society for Magnetic Resonance in Medicine, Hawaii, USA, p. 1224.
Fjell, A.M., Westlye, L.T., Greve, D.N., Fischl, B., Benner, T., van der Kouwe, A.J., Salat, D., Bjørnerud, A., Due-Tønnessen, P., Walhovd, K.B., 2008. The relationship between diffusion tensor imaging and volumetry as measures of white matter properties. Neuroimage 42 (4), 1654–1668.
Frank, L.R., 2001. Anisotropy in high angular resolution diffusion-weighted MRI. Magn. Reson. Med. 45 (6), 935–939.
Hasan, K.M., Iftikhar, A., Kamali, A., Kramer, L.A., Ashtari, M., Cirino, P.T., Papanicolaou, A.C., Fletcher, J.M., Ewing-Cobbs, L., 2009. Development and aging of the healthy human brain uncinate fasciculus across the lifespan using diffusion tensor tractography. Brain Res. 1276, 67–76.
Hsu, J.-L., Leemans, A., Bai, C.-H., Lee, C.-H., Tsai, Y.-F., Chiu, H.-C., Chen, W.-H., 2008. Gender differences and age-related white matter changes of the human brain: a diffusion tensor imaging study. Neuroimage 39 (2), 566–577.
Hsu, J.-L., Van Hecke, W., Bai, C.-H., Lee, C.-H., Tsai, Y.-F., Chiu, H.-C., Jaw, F.-S., Hsu, C.-Y., Leu, J.-G., Chen, W.-H., Leemans, A., 2010. Microstructural white matter changes in normal aging: a diffusion tensor imaging study with higher-order polynomial regression models. Neuroimage 49 (1), 32–43.
Huang, H., Zhang, J., Wakana, S., Zhang, W., Ren, T., Richards, L.J., Yarowsky, P., Donohue, P., Graham, E., van Zijl, P.C., Mori, S., 2006. White and gray matter development in human fetal, newborn and pediatric brains. Neuroimage 33 (1), 27–38.
Huster, R.J., Westerhausen, R., Kreuder, F., Schweiger, E., Wittling, W., 2009. Hemispheric and gender related differences in the midcingulum bundle: a DTI study. Hum. Brain Mapp. 30 (2), 383–391.
Jones, D.K., Basser, P.J., 2004. Squashing peanuts and smashing pumpkins: how noise distorts diffusion-weighted MR data. Magn. Reson. Med. 52 (5), 979–993.
Jones, D.K., Catani, M., Pierpaoli, C., Reeves, S.J., Shergill, S.S., O'Sullivan, M., Golesworthy, P., McGuire, P., Horsfield, M.A., Simmons, A., Williams, S.C., Howard, R.J., 2006. Age effects on diffusion tensor magnetic resonance imaging tractography measures of frontal cortex connections in schizophrenia. Hum. Brain Mapp. 27 (3), 230–238.
Jones, D.K., Horsfield, M., Simmons, A., 1999a. Optimal strategies for measuring diffusion in anisotropic systems by magnetic resonance imaging. Magn. Reson. Med. 42 (3), 515–525.
Jones, D.K., Lythgoe, D., Horsfield, M.A., Simmons, A., Williams, S.C.R., Markus, H.S., 1999b. Characterization of white matter damage in ischemic leukoaraiosis with diffusion tensor MRI. Stroke 30 (2), 393–397.
Jones, D.K., Travis, A.R., Eden, G., Pierpaoli, C., Basser, P.J., 2005. PASTA: pointwise assessment of streamline tractography attributes. Magn. Reson. Med. 53 (6), 1462–1467.
Klein, S., Staring, M., Murphy, K., Viergever, M.A., Pluim, J., 2010. Elastix: a toolbox for intensity-based medical image registration. IEEE Trans. Med. Imaging 29, 196–205.
Le Bihan, D., Mangin, J.-F., Poupon, C., Clark, C.A., Pappata, S., Molko, N., Chabriat, H., 2001. Diffusion tensor imaging: concepts and applications. J. Magn. Reson. Imaging 13 (4), 534–546.
Lebel, C., Caverhill-Godkewitsh, S., Beaulieu, C., 2010. Age-related regional variations of the corpus callosum identified by diffusion tensor tractography. NeuroImage 52 (1), 20–31.
Lebel, C., Walker, L., Leemans, A., Phillips, L., Beaulieu, C., 2008. Microstructural maturation of the human brain from childhood to adulthood. Neuroimage 40 (3), 1044–1055.
Leemans, A., Jeurissen, B., Sijbers, J., Jones, D.K., 2009. ExploreDTI: a graphical toolbox for processing, analyzing, and visualizing diffusion MR data. Proceedings of the 17th Annual Meeting of International Society for Magnetic Resonance in Medicine, Hawaii, USA, p. 3536.
Leemans, A., Jones, D.K., 2009. The B-matrix must be rotated when correcting for subject motion in DTI data. Magn. Reson. Med. 61 (6), 1336–1349.
Leemans, A., Sijbers, J., Verhoye, M., van der Linden, A., van Dyck, D., 2005. Mathematical framework for simulating diffusion tensor MR neural fiber bundles. Magn. Reson. Med. 53 (4), 944–953.
Liu, R.S.N., Lemieux, L., Bell, G.S., Sisodiya, S.M., Shorvon, S.D., Sander, J.W.A.S., Duncan, J.S., 2003. A longitudinal study of brain morphometrics using quantitative magnetic resonance imaging and difference image analysis. Neuroimage 20 (1), 22–33.
Madden, D., Bennett, I., Song, A., 2009. Cerebral white matter integrity and cognitive aging: contributions from diffusion tensor imaging. Neuropsychol. Rev. 19 (4), 415–435 Dec.
Malykhin, N., Concha, L., Seres, P., Beaulieu, C., Coupland, N.J., 2008. Diffusion tensor imaging tractography and reliability analysis for limbic and paralimbic white matter tracts. Psychiatry Res. Neuroimaging 164 (2), 132–142.
Marquardt, D., 1963. An algorithm for least-squares estimation of nonlinear parameters. J. Soc. Ind. Appl. Math. 11, 431–441.
Mori, S., Crain, B.J., Chacko, V.P., Zijl, P.C.M.V., 1999. Three-dimensional tracking of axonal projections in the brain by magnetic resonance imaging. Ann. Neurol. 45 (2), 265–269.
Mukherjee, P., Miller, J.H., Shimony, J.S., Conturo, T.E., Lee, B.C.P., Almli, C.R., McKinstry, R.C., 2001. Normal brain maturation during childhood: developmental trends characterized with diffusion-tensor MR imaging. Radiology 221 (2), 349–358.
Oouchi, H., Yamada, K., Sakai, K., Kizu, O., Kubota, T., Ito, H., Nishimura, T., 2007. Diffusion anisotropy measurement of brain white matter is affected by voxel size: underestimation occurs in areas with crossing fibers. AJNR Am. J. Neuroradiol. 28 (6), 1102–1106.
Otsu, N., 1979. A threshold selection method from gray-level histograms. IEEE Trans. Syst. Man Cybern. 9 (1), 62–66 January.
Papadakis, N.G., Martin, K.M., Mustafa, M.H., Wilkinson, I.D., Griffiths, P.D., Huang, C.L.-H., Woodruff, P.W., 2002. Study of the effect of CSF suppression on white matter diffusion anisotropy mapping of healthy human brain. Magn. Reson. Med. 48 (2), 394–398.
Pasternak, O., Sochen, N., Gur, Y., Intrator, N., Assaf, Y., 2009. Free water elimination and mapping from diffusion MRI. Magn. Reson. Med. 62 (3), 717–730.
Pfefferbaum, A., Sullivan, E.V., 2003. Increased brain white matter diffusivity in normal adult aging: relationship to anisotropy and partial voluming. Magn. Reson. Med. 49 (5), 953–961.
Pierpaoli, C., Barnett, A., Pajevic, S., Chen, R., Penix, L., Virta, A., Basser, P.J., 2001. Water diffusion changes in Wallerian degeneration and their dependence on white matter architecture. Neuroimage 13 (6), 1174–1185.

Pierpaoli, C., Jezzard, P., Basser, P.J., Barnett, A., Di Chiro, G., 1996. Diffusion tensor MR imaging of the human brain. Radiology 201 (3), 637–648.
Pierpaoli, C., Jones, D.K., 2004. Removing CSF contamination in brain DT-MRIs by using a two-compartment tensor model. Proceedings of the 12th Annual Meeting of International Society for Magnetic Resonance in Medicine, Kyoto, Japan, p. 1215.
Pluim, J.P.W., Maintz, J.B.A., Viergever, M.A., 2003. Mutual-information-based registration of medical images: a survey. IEEE Trans. Med. Imaging 22 (8), 986–1004.
Resnick, S.M., Pham, D.L., Kraut, M.A., Zonderman, A.B., Davatzikos, C., 2003. Longitudinal magnetic resonance imaging studies of older adults: a shrinking brain. J. Neurosci. 23 (8), 3295–3301.
Rohde, G.K., Barnett, A.S., Basser, P.J., Marenco, S., Pierpaoli, C., 2004. Comprehensive approach for correction of motion and distortion in diffusion-weighted MRI. Magn. Reson. Med. 51 (1), 103–114.
Sala, S., Agosta, F., Pagani, E., Copetti, M., Comi, G., Filippi, M., in Press. Microstructural changes and atrophy in brain white matter tracts with aging. Neurobiol. Aging. doi:10.1016/j.neurobiolaging.2010.04.027.
Salat, D.H., Tuch, D., Greve, D.N., van der Kouwe, A.J.W., Hevelone, N.D., Zaleta, A.K., Rosen, B., Fischl, B., Corkin, S., Rosas, H.D., Dale, A.M., 2005. Age-related alterations in white matter microstructure measured by diffusion tensor imaging. Neurobiol. Aging 26 (8), 1215–1227.
Song, S.-K., Sun, S.-W., Ju, W.-K., Lin, S.-J., Cross, A.H., Neufeld, A.H., 2003. Diffusion tensor imaging detects and differentiates axon and myelin degeneration in mouse optic nerve after retinal ischemia. Neuroimage 20 (3), 1714–1722.
Song, S.-K., Sun, S.-W., Ramsbottom, M.J., Chang, C., Russell, J., Cross, A.H., 2002. Dysmyelination revealed through MRI as increased radial (but unchanged axial) diffusion of water. Neuroimage 17 (3), 1429–1436.
Taoka, T., Morikawa, M., Akashi, T., Miyasaka, T., Nakagawa, H., Kiuchi, K., Kishimoto, T., Kichikawa, K., 2009. Fractional anisotropy-threshold dependence in tract-based diffusion tensor analysis: evaluation of the uncinate fasciculus in Alzheimer disease. AJNR Am. J. Neuroradiol. 30 (9), 1700–1703.
Tournier, J.-D., Calamante, F., Gadian, D.G., Connelly, A., 2004. Direct estimation of the fiber orientation density function from diffusion-weighted MRI data using spherical deconvolution. Neuroimage 23 (3), 1176–1185.
Tuch, D.S., 2004. Q-ball imaging. Magn. Reson. Med. 52 (6), 1358–1372.
Voineskos, A.N., Lobaugh, N.J., Bouix, S., Rajji, T.K., Miranda, D., Kennedy, J.L., Mulsant, B.H., Pollock, B.G., Shenton, M.E., 2010. Diffusion tensor tractography findings in schizophrenia across the adult lifespan. Brain 133, 1494–1504.
Voineskos, A.N., Rajji, T.K., Lobaugh, N.J., Miranda, D., Shenton, M.E., Kennedy, J.L., Pollock, B.G., Mulsant, B.H., in Press. Age-related decline in white matter tract integrity and cognitive performance: A DTI tractography and structural equation modeling study. Neurobiol. Aging. doi:10.1016/j.neurobiolaging.2010.02.009.
Vos, S.B., Viergever, M.A., Jones, D.K., Leemans, A., 2010. Partial volume effect as a hidden covariate in tractography based analyses of fractional anisotropy: does size matter? Proceedings of the 18th Annual Meeting of International Society for Magnetic Resonance in Medicine. Stockholm, Sweden, p. 113.
Westlye, L.T., Walhovd, K.B., Dale, A.M., Bjornerud, A., Due-Tonnessen, P., Engvig, A., Grydeland, H., Tamnes, C.K., Ostby, Y., Fjell, A.M., 2009. Life-span changes of the human brain white matter: diffusion tensor imaging (DTI) and volumetry. Cereb. Cortex 20 (9), 2055–2068.
Wilson, M., Tench, C.R., Morgan, P.S., Blumhardt, L.D., 2003. Pyramidal tract mapping by diffusion tensor magnetic resonance imaging in multiple sclerosis: improving correlations with disability. J. Neurol. Neurosurg. Psychiatry 74 (2), 203–207.
Yoshiura, T., Wu, O., Zaheer, A., Reese, T.G., Sorensen, A.G., 2001. Highly diffusion-sensitized MRI of brain: dissociation of gray and white matter. Magn. Reson. Med. 45 (5), 734–740.